

CrystEngComm

Accepted Manuscript



This is an *Accepted Manuscript*, which has been through the Royal Society of Chemistry peer review process and has been accepted for publication.

Accepted Manuscripts are published online shortly after acceptance, before technical editing, formatting and proof reading. Using this free service, authors can make their results available to the community, in citable form, before we publish the edited article. We will replace this *Accepted Manuscript* with the edited and formatted *Advance Article* as soon as it is available.

You can find more information about *Accepted Manuscripts* in the [Information for Authors](#).

Please note that technical editing may introduce minor changes to the text and/or graphics, which may alter content. The journal's standard [Terms & Conditions](#) and the [Ethical guidelines](#) still apply. In no event shall the Royal Society of Chemistry be held responsible for any errors or omissions in this *Accepted Manuscript* or any consequences arising from the use of any information it contains.

Dramatic Shape Transformation of Ag Nanoparticles with Concave Facets in a Solvothermal Process

Received 00th January 20xx,
Accepted 00th January 20xx

Qiang Zhang*, Kunyu Dong, Changping Wang and Yiyun Cheng*

DOI: 10.1039/x0xx00000x

www.rsc.org/

Tailoring the morphologies of metal nanoparticles especially that with concave facets is still a big challenge for the current syntheses. Here, we reported a facile and robust approach for the synthesis of Ag nanoparticles with different morphologies and concave facets.

Manipulating the morphologies of metal nanoparticles gives significant impact to their optical, catalytic, magnetic, and electronic properties.¹ For instant, the optical properties of gold nanoparticles can be tuned in a broad range from the visible to near-infrared region by changing the shell thicknesses for nanoshells,² the aspect ratios for nanorods³ and the interior cavities for nanocages,⁴ while the catalytic activity of platinum and palladium nanoparticles are strongly dependent on their size, shapes, and concave features.⁵ Silver (Ag) nanoparticles with well-defined geometries have attracted tremendous interest in recent years due to their unique optical properties and applications related to the localized surface plasmon resonance (LSPR)⁶ and surface-enhanced Raman scattering (SERS)⁷ and also their nature as a sacrificial template to synthesis hollowed noble metal nanostructures for diverse applications such as catalysis,⁸ bio-imaging,⁹ photothermal therapy,¹⁰ and drug delivery.¹¹ Ag nanoparticles with concave facets also exhibit their superiorities for the tunable LSPR peaks and enhanced SERS activities.¹² However, few of methods have been developed to synthesize Ag nanoparticles with concave facets until now. Yang and coworkers firstly reported an anisotropic etching method to produce octahedra and octapods with concave facets.^{12a} Xia et al described a seed-mediated method to prepare Ag nanocrystals with concave facets including octahedra, cubes, octapods and trisoctahedra.^{12b} In this study, we described a facile method to prepare diverse Ag nanoparticles with concave facets, which simply involved a solvothermal heating of Ag nanoparticles in ethanol

dissolved with polyvinyl pyrrolidone of ~29000 Da (PVP29K).

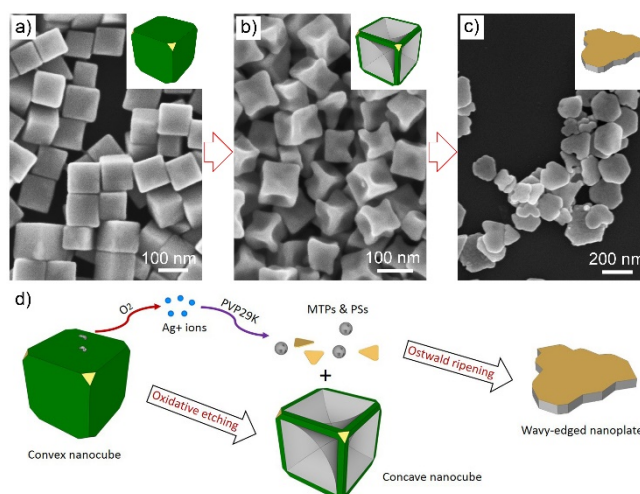


Fig. 1 Shape evolution of Ag nanoparticles in a typical solvothermal process. a) Original Ag nanocubes, b) Ag nanocubes with concave facets and c) wavy-edged Ag nanoplates obtained at a reaction time point of 0, 6 and 12 h, respectively. d) A possible mechanism for the shape transformation of Ag nanoparticles in the solvothermal process.

In a typical synthesis, a mix of 10 mL PVP29K (1mM) and 0.5 mL Ag nanocubes (2.2×10^{13} particles/L) in ethanol was sealed in a Teflon liner in autoclave, and then was heated at 80 °C for 6 h (see the details in Supporting Information). The distinguishing nanostructures obtained from the syntheses stopped at different times were shown in Fig. 1. The initial nanoparticles, Ag nanocubes, dramatically transformed into nanocubes with concave facets and then wavy-edged nanoplates, when the reactions were stopped at a time point of 6 and 12 h, respectively. The scanning electron microscopy (SEM) image shows that nanoparticles obtained at 6 h had dark contrast in their {100} surfaces (Fig. 1b), and the transmission electron microscopy (TEM) image shows that these nanoparticles had light contrast in the surface centers and the edges (Fig. 2a), both of which suggest that the nanoparticles obtained at 6 h were Ag nanocubes with concave facets. Furthermore, the low

Shanghai Key Laboratory of Regulatory Biology, School of Life Sciences, East China Normal University, Shanghai 200062, P. R. China. Email: yucheng@mail.ustc.edu.cn (Y. C.) and qzhang@bio.ecnu.edu.cn (Q. Z.)

Electronic Supplementary Information (ESI) available. See DOI: 10.1039/x0xx00000x

magnification SEM image suggests that the as-obtained Ag nanocubes with concave facets were high quality and high yield (nearly 100 %) (Fig. S1). To further evaluate their concave nature, individual Ag nanocube with concave facets projected along different directions including $\langle 100 \rangle$, $\langle 110 \rangle$, and $\langle 111 \rangle$ axis were displayed in Fig. 2b-d (from up to bottom). Particles sit in different orientations suggest the formation of cavities in the six $\{100\}$ surfaces. If terminating the reaction at 12 h, Ag nanocubes turned into wavy-edged nanoplates of triangular and hexagonal shapes (Fig. 1c). The homogenous contrast on their $\{111\}$ facets indicates that their surfaces were convex, while the wavy-like edges suggest their boundaries were composed of high-index facets.

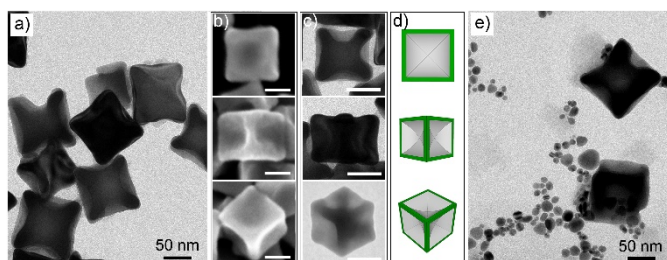


Fig. 2 Ag nanocubes with concave facets obtained at a reaction time point of 6 h. a) Ag nanocubes with concave facets collected by centrifuging the fresh reaction solution at 15000 rpm for 10 min. b) SEM, c) TEM, and d) model images of a typical Ag nanocube with concave facets orientated along $\langle 100 \rangle$ (top panel), $\langle 110 \rangle$ (middle panel), and $\langle 111 \rangle$ (bottom panel) direction, respectively. The scale bars in panel a) and b) are 50 nm. e) Ag nanocubes with concave facets and MTPs and PSs collected by centrifuging the fresh reaction solution at 55000 rpm for 30 min.

The nanocubes with concave facets shown in Fig. 1b and 2a were collected from the solid from the reaction solution centrifuged at 15000 revolutions per min (rpm) for 10 min. However, the removed supernatant still represented a slight yellow color, which indicates ultrasmall nanoparticles in it. To identify the component in the supernatant, the fresh reaction solution was centrifuged at a higher rate of 55000 rpm for 30 min. The supernatant became clear, and the solid was analyzed by TEM. As shown in Fig. 2e, Ag nanocubes with concave facets were co-existed with the ultrasmall nanoparticles including multiple-twinned nanoparticles (MTPs) and plate-like seeds (PSs). This result suggests that an etching mechanism should take responsibility for the shape transformation of Ag nanocubes into the ones with concave facets. If the reaction was continued for 12 h, these MTPs and PSs were finally transformed into wavy-edged nanoplates. This phenomenon is quite consistent with our previous study for the solvothermal synthesis of Ag nanoplates,¹³ in which silver nitrate was initially reduced into MTPs and PSs, and then MTPs were dissolved and PSs grew up into Ag nanoplates via O_2 -mediated Ostwald ripening, indicating the transformation from MTPs and PSs into wavy-edged nanoplates in this case also underwent the similar Ostwald ripening process.

In order to clarify the mechanism for shape transformation, we conducted a series of typical reactions and stopped them at different time points of 2, 4, 6, and 8 h, respectively (Fig. S2). Compared with the original Ag nanocubes (Fig. 1a), Ag nanoparticles obtained at 2 h

had an inhomogenous contrast on their surfaces and slight curvatures on their edges, indicating small pits arisen in the $\{100\}$ facets (Fig. S2a), while when the particles were heated for 4 h, the small pits were connected and developed into cavities (Fig. S2b). If the reaction terminated at 6 h, the typical Ag nanocubes with deep cavities in their surfaces were obtained (Fig. S2c). If the reaction stopped at 8 h, the Ag nanocubes with concave facets became into broken nanoframes, and Ag nanoplates emerged in the product (Fig. S2d). The corresponding ultraviolet and visible (UV-Vis) spectra for the reactions stopped at different times were recorded (Fig. S2e). Compared with the original Ag nanocubes, the LSPR peaks of Ag nanocubes with concave facets obtained at 2 and 4 h were red-shifted plus with increased intensities. The broad peaks arisen at the wavelength of 500-800 nm were mainly attributed to the enhanced scattering of the structures with concave facets. The significantly increased peak intensity at 800 nm for the sample obtained at 8 h owing to the generation of Ag nanoplates. The gradually arisen narrow peaks at ~ 400 nm for the samples obtained at 4 and 6 h attributed to the generation of MTPs and PSs, which further disappeared in the sample obtained at 8 h, indicating the MTPs and PSs were converted into Ag nanoplates. Moreover, the inductively coupled plasma mass spectrometer (ICP-MS) was employed to analyze the Ag contents in the supernatants and the solids that separated via high-speed centrifugation at 55000 rpm for 30 min. Although there still might be few ultrasmall Ag nanoparticles co-existed with ionic Ag in the supernatant, the extremely low Ag concentration in which suggests that the etched Ag atoms from Ag nanocubes majorly converted into MTPs and PSs (Fig. S2f).

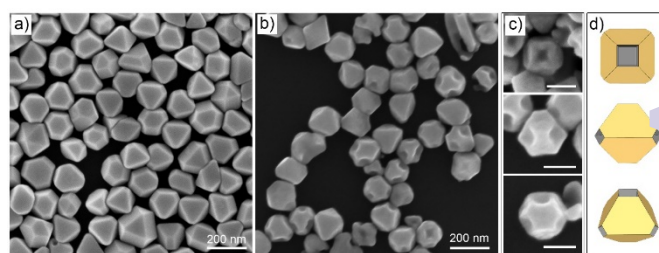


Fig. 3 Shape transformation of Ag cubo-octahedra in the solvothermal process. a) Original Ag cubo-octahedra. b) Ag cubo-octahedra with concave facets obtained after solvothermal treatment for 6 h. c) and d) SEM and model images of Ag cubo-octahedra with concave facets orientated along $\langle 100 \rangle$ (top panel), $\langle 110 \rangle$ (middle panel), and $\langle 111 \rangle$ (bottom panel) direction, respectively. The scale bars in panel c) are 100 nm.

The original Ag nanocubes had few by-product, bipyramids, co-existed with them, and after the typical solvothermal treatment for 6 h, these bipyramids also converted into structures with cavities in their $\{100\}$ surfaces (Fig. S3). This result suggests the solvothermal treatment could be developed into a universal method to prepare Ag nanoparticles with concave facets and diverse shapes. Moreover, the examples of Ag nanocubes and bipyramids indicate that the $\{100\}$ surfaces were preferentially etched in the solvothermal process. To identify the two conjectures, we further treated Ag cubo-octahedra with the same solvothermal heating, which were mainly covered by comparable $\{100\}$ and $\{111\}$ facets (Fig. 3a). As we presumed, Ag cubo-octahedra became into nanoparticles with concave facets after

solvothermal treatment for 6 h (Fig. 3b), and their {100} facets were preferentially etched compared with their {111} facets. The individual particle sit in different orientations suggests that the {100} facets of cuboctahedra were all excavated into cavities, and their {111} facets were all convex (Fig. 3c and d). The preferential etching in {100} facets was consistent with the previous study by Yang et al.,^{12a} which suggests that a suitable etchant selective for high-energy surfaces allows the introduction of anisotropy into nanoparticles. In this case, {100} facets were high surface energy compared with {111} facets,¹⁴ thus leading to an anisotropic etching to create structures with concave facets.

The standard reaction was processed in an isolated system with high temperature and high-pressure. To verify if the high pressure played a critical role in the shape transformation, we conducted the typical synthesis in an opened flask at 80 °C, which was equipped with condenser pipe to prevent the evaporation of ethanol. The as-obtained products were also composed of Ag nanocubes with concave facets and random nanoparticles (Fig. S4). However, these Ag nanocubes were slightly concave compared with the one obtained from typical solvothermal synthesis, and the random nanoparticles had a relative larger size than the ones generated in the solvothermal synthesis, which makes it difficult to separate them from Ag nanocubes with concave facets via centrifugation. This result suggests that the high pressure was critical essential for the preparation of high quality of Ag nanoparticles with concave facets.

In this case, it is suggested that the Ag nanoparticles with concave facets were generated via an etching process, thus an etchant must exist in the reaction system. In a typical synthesis, the only possible etchant was oxygen (O₂) that was from the dissolved O₂ in ethanol and the air sealed in the Teflon liner. We conducted the typical reaction in a flask with the protection of argon. The as-generated Ag nanoparticles were not structures with concave facets (Fig. S5), indicating O₂ indeed played a role of oxidative etchant in this synthesis. Both the TEM image (Fig. 2e) and ICP-MS analysis (Fig. S2f) suggests that the ionic Ag majorly converted into MTPs and PSs. Thus, there should also be a reductant in this synthesis. PVP terminated with hydroxyl group was suggested to have a mild reducing power and have been widely used for the synthesis of metal nanoparticles.¹⁵ Therefore, we conducted a synthesis without the addition of PVP29K and observed that Ag nanocubes didn't convert into structures with concave facets (Fig. S6), which suggests that PVP29K was indeed the reductant in this case. Furthermore, we performed the syntheses with the addition of PVP of ~10000 and ~55000 Da (PVP10K and PVP55K) instead of PVP29K. However, Ag nanocubes in the synthesis with PVP10K had no morphology changes, while the sample collected from the reaction with PVP55K became into truncated Ag nanocubes on their corners and edges (Fig. S7). The previous studies suggest that PVP terminated with hydroxyl groups not only plays a critical role in the control of the particle morphologies¹⁶ but also can serve as a reductant for the synthesis of metal nanoparticles, and moreover PVP with smaller molecular weight has a relative stronger reducing ability.^{15,17} Therefore, in this case, PVP10K could efficiently prevent the O₂-induced detachment of Ag atom from Ag nanocubes due to their relative strong reducing power, which is further confirmed by adding another strong reductant, ascorbic acid, in two reactions without and with the

presence of PVP29K (Fig. S8 a and b, respectively). PVP55K had a relative weak reducing power compared with PVP10K and PVP29K, and thus it couldn't prevent the O₂-mediated detachment of Ag atoms from the {100} facets of Ag nanocubes or also couldn't reduce the O₂-mediated Ag etching from the {111} and {110} facets on the corners and edges of Ag nanocubes, which consequently resulted in an isotropic etching over the surfaces, edges and corners of Ag nanocubes. These results suggest that an appropriate etching pair (in this case, O₂ and PVP29K) was critical for the anisotropic etching, which is quite consistent with the investigation by Yang and coworkers.^{12a} Taken together, a reasonable mechanism was proposed in Fig. 1b. Ag nanoparticles (nanocubes as a model) were facet-selectively etched by an etching pair of O₂ and PVP29K and then were transformed into concave nanoparticles, and the by-product of MTPs and PSs further underwent an Ostwald-ripening process to generate the wavy-edged nanoplates.

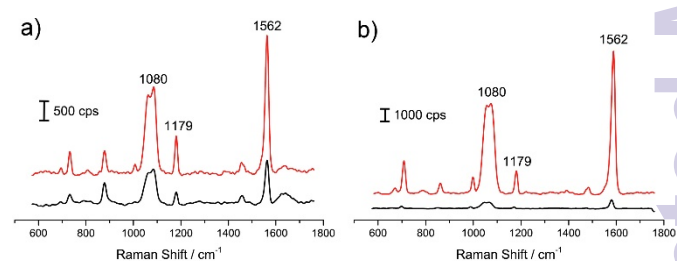


Fig. 4 SERS activity of Ag nanocubes with concave facets. The SERS spectra of 1,4-BDT absorbed on the surface of Ag nanocubes (black curve) and Ag nanocubes with concave facets (red curve) were acquired with laser at wavelength of a) 530 and b) 785 nm, respectively.

The SERS activity of Ag nanocubes with concave facets was also evaluated. Compared with the normal Ag nanocubes, Ag nanocubes with concave facets represented a much higher SERS activity (Fig. 4). The surface cavities of Ag nanocubes with concave facets and the increased sharp corners and edges were supposed to create new hot spots for the enhanced SERS activity (Fig. 4). Moreover, Raman signals acquired from laser irradiation at 785 nm showed enhanced SERS signal compared that acquired from laser irradiation at 530 nm (Fig. 4), which is attributed to the arisen LSPR peaks for Ag nanocubes with concave facets in the near-infrared region.

In summary, we reported a facile solvothermal synthesis in which Ag nanocubes dramatically transformed into nanocubes with concave facets and finally wavy-edged nanoplates. The method was further explored as a routine method to fabricate Ag nanoparticles with concave facets and diverse shapes. The anisotropic etching activity for generating Ag nanoparticles with concave facets was owing to the dissimilar surface energies of Ag nanoparticles and the existence of a suitable etching pair (e.g. O₂ and PVP29K), and the generation of wavy-edged nanoplates was due to the well-known Ostwald ripening occurred between the in-situ generated MTPs and PSs. The as-prepared Ag nanocubes with concave facets showed a tunable concavities and red-shifted LSPR peaks and significantly enhanced SERS activity. Taken together, this investigation offered a robust method to prepare Ag nanoparticles with concave facets and diverse shapes.

This research was financially supported by the National Natural Science Foundation of China (Grant No. 21207038), the Research Found for the Doctoral Program of Higher Education of China (Grant No. 20120076120027), the Shanghai Pujiang Program (Grant No.14PJD016), and the Shanghai Chenguang Program (Grant No. 12CG25).

Notes and references

1. T. Shegai, Z. Li, T. Dadosh, Z. Zhang, H. Xu and G. Haran, *Proc. Natl. Acad. Sci. U S A*, 2008, **105**, 16448; (b) C. Cui, L. Gan, M. Heggen, S. Rudi and P. Strasser, *Nat. Mater.*, 2013, **12**, 765; (c) J. Gao, H. Gu and B. Xu, *Acc. Chem. Res.*, 2009, **42**, 1097; (d) I. Park, S. H. Ko, H. Pan, C. P. Grigoropoulos, A. P. Pisano, J. M. Fréchet, E. S. Lee and J. H. Jeong, *Adv. Mater.*, 2008, **20**, 489.
2. E. Prodan, P. Nordlander and N. Halas, *Nano Lett.*, 2003, **3**, 1411.
3. B. D. Busbee, S. O. Obare and C. J. Murphy, *Adv. Mater.*, 2003, **15**, 414.
4. S. E. Skrabalak, J. Chen, Y. Sun, X. Lu, L. Au, C. M. Cobley and Y. Xia, *Acc. Chem. Res.*, 2008, **41**, 1587.
5. (a) S. Mostafa, F. Behafarid, J. R. Croy, L. K. Ono, L. Li, J. C. Yang, A. I. Frenkel and B. R. Cuenya, *J. Am. Chem. Soc.*, 2010, **132**, 15714; (b) M. Jin, H. Zhang, Z. Xie and Y. Xia, *Angew. Chem. Int. Edit.*, 2011, **50**, 7850; (c) C. Wang, H. Daimon, T. Onodera, T. Koda and S. Sun, *Angew. Chem. Int. Edit.*, 2008, **47**, 3588.
6. (a) L. J. Sherry, S.-H. Chang, G. C. Schatz, R. P. Van Duyne, B. J. Wiley and Y. Xia, *Nano Lett.*, 2005, **5**, 2034; (b) A. D. McFarland and R. P. Van Duyne, *Nano Lett.*, 2003, **3**, 1057.
7. (a) X.-M. Qian and S. Nie, *Chem. Soc. Rev.*, 2008, **37**, 912; (b) D. Jana, A. Mandal, G. De, *ACS Appl. Mater. Interfaces* 2012, **4**, 3330.
8. J. Zeng, Q. Zhang, J. Chen and Y. Xia, *Nano Lett.*, 2009, **10**, 30.
9. L. Tong, C. M. Cobley, J. Chen, Y. Xia and J. X. Cheng, *Angew. Chem. Int. Edit.*, 2010, **49**, 3485.
10. L. Au, D. Zheng, F. Zhou, Z.-Y. Li, X. Li and Y. Xia, *ACS nano*, 2008, **2**, 1645.
11. F. Hu, Y. Zhang, G. Chen, C. Li and Q. Wang, *Small*, 2015, **11**, 985.
12. (a) M. J. Mulvihill, X. Y. Ling, J. Henzie and P. Yang, *J. Am. Chem. Soc.*, 2009, **132**, 268; (b) X. Xia, J. Zeng, B. McDearmon, Y. Zheng, Q. Li and Y. Xia, *Angew. Chem.*, 2011, **123**, 12750.
13. Q. Zhang, Y. Yang, J. Li, R. Iurilli, S. Xie and D. Qin, *ACS Appl. Mater. Interfaces*, 2013, **5**, 6333.
14. A. Tao, P. Sinsermsuksakul and P. Yang, *Angew. Chem. Int. Edit.*, 2006, **45**, 4597.
15. Y. Xiong, I. Washio, J. Chen, H. Cai, Z.-Y. Li and Y. Xia, *Langmuir*, 2006, **22**, 8563.
16. (a) M. Rycenga, C.M. Cobley, J. Zeng, W. Li, C. Moran, Q. Zhang, D. Qin, Y. Xia, *Chem. Res.* 2011, **111**, 3669; (b) D. Jana, G. De, *J. Mater. Chem.*, 2011, **21**, 6072.
17. I. Washio, Y. Xiong, Y. Yin and Y. Xia, *Adv. Mater.*, 2006, **18**, 1745.